Targeted Oxidation Strategy (TOS) for Potential Inhibition of Coronaviruses by Disulfiram — a 70-year Old Anti-alcoholism Drug

Luyan Xu[1,4,5,7, §], Jiahui Tong [2,3,6,7, §], Yiran Wu[2], Suwen Zhao[2,3,*], Bo-Lin Lin[1, 4,5,7,*]

1. School of Physical Science and Technology, ShanghaiTech University, Shanghai 201210, China

2. iHuman Institute, ShanghaiTech University, Shanghai 201210, China

3. School of Life Science and Technology, ShanghaiTech University, Shanghai 201210, China

4. Shanghai Advanced Research Institute, Chinese Academy of Sciences, Shanghai 201210, China

5. Shanghai Institute of Organic Chemistry, Chinese Academy of Sciences, Shanghai 200032, China

6. Key Laboratory of Computational Biology, CAS-MPG Partner Institute for Computational Biology, Shanghai Institutes for Biological Sciences, Chinese Academy of Sciences, Shanghai, 200031, China

7. University of Chinese Academy of Sciences, Beijing 100049, China

[§]**Co-first authors**.

*Corresponding author email addresses: zhaosw@shanghaitech.edu.cn,

linbl@shanghaitech.edu.cn.

Abstract

In the new millennium, the outbreak of new coronavirus has happened three times: SARS-CoV, MERS-CoV, and 2019-nCoV. Unfortunately, we still have no pharmaceutical weapons against the diseases caused by these viruses. The pandemic of 2019-nCoV reminds us of the urgency to search new drugs with totally different mechanism that may target the weaknesses specific to coronaviruses. Herein, we disclose a new targeted oxidation strategy (TOS II) leveraging non-covalent interactions potentially to oxidize and inhibit the activities of cytosolic thiol proteins via thiol/thiolate oxidation to disulfide (TOD). Quantum mechanical calculations show encouraging results supporting the feasibility to selectively oxidize thiol of targeted proteins via TOS II even in relatively reducing cytosolic microenvironments. Molecular docking against the two thiol proteases M^{pro} and PL^{pro} of 2019-nCoV provide evidence to support a TOS II mechanism for two experimentally identified anti-2019-nCoV disulfide oxidants: disulfiram and PX-12. Remarkably, disulfiram is an anti-alcoholism drug approved by FDA 70 years ago, thus it can be immediately used in phase III clinical trial for anti-2019-nCoV treatment. Finally, a preliminary list of promising TOS II drug candidates targeting the two thiol proteases of 2019-nCoV are proposed upon virtual screening of 32143 disulfides.

Introduction

Aggressive RNA viruses are typically characterized by rapid reproductive activities in cytoplasm. Similar to normal cells, proliferations of contagious RNA coronaviruses, including SARS-CoV, MERS-CoV and 2019-nCoV, heavily rely on the functions of proteins containing crucial thiol/zinc(II)-thiolate sites, such as thiol protease and RNA replicase. Thus, thiol/thiolate oxidation to disulfide (TOD) caused by appropriate oxidants may transform the proteins from primitive active form to targeted inactive form (**Fig. 1A**), providing a potential new strategy to block the life cycle of RNA viruses.
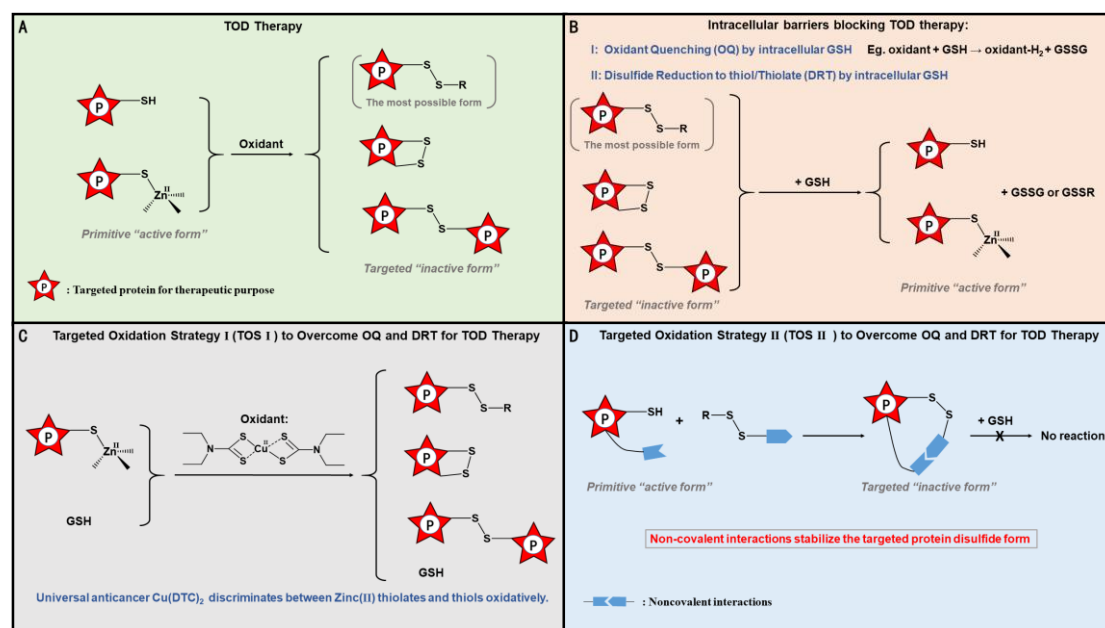
Figure 1. Schematics illustrating the principle for target oxidation strategy (TOS): A. Thiol/thiolate oxidation to disulfide (TOD) caused by appropriate oxidants to transform proteins from primitive active form to targeted inactive form; B. Oxidant quenching (OD) and disulfide reduction to thiol/thiolate (DRT) blocking intracellular TOD; C. TOS I to overcome OD and DRT for TOD therapy; D. TOS II to overcome

OD and DRT for TOD therapy.

However, such strategy is generally disabled by an intracellular reductive environment common in aerobic organisms, which is regulated by glutathione (GSH) in mM concentrations and high ratios of GSH to GSSG (glutathione disulfide, an oxidized form of GSH) in cytoplasm[1, 2] (**Fig. 1B**). Oxidant quenching (OQ) by GSH can lower the accessibility of thiol/zinc(II)-thiolate sites of cytosolic proteins to oxidants to a relatively non-deleterious level. Additionally, disulfide reduction to thiol/thiolate (DRT) by GSH in local cytosolic microenvironments with high GSH:GSSG ratios (*ca.* 30-100[3]) can restore the primitive active form of proteins even if aberrant TOD occurs occasionally. We postulated that such combination of OQ and DRT may likely be an essential reductive-protection mechanism evolved by aerobic organisms to reconcile the conflicting vital needs of both oxygen and oxidatively-unstable intracellular functional sites as a response to the transition from an O_2-lean atmosphere to an O_2-rich one on ancient Earth. Consequently, how to overcome OQ/DRT on demand represents a key challenge for potential therapeutic applications of TOD, such as killing malignant cells and inhibiting cytosolic proliferation of RNA viruses *in vivo*.

Recently, we reported that targeted oxidation strategy (TOS I, **Fig. 1C**) can allow oxidants to avoid OQ and lead to intracellular TOD, unraveling a new general chemical mechanism for the universal anticancer activities of disulfiram and its

metabolite $Cu(DTC)_2$. The coordination of DTC tunes the oxidation ability of Cu(II) abnormally pre-accumulated in tumors just to the right level between the oxidation potentials of thiol and zinc(II) thiolate. Thus, the classical redox reactivity between Cu(II) and thiol is blocked while the ability to oxidize proteins containing zinc(II)-thiolate site to the corresponding disulfide form is preserved by $Cu(DTC)_2$, resulting in targeted oxidative damage of intracellular zinc-finger domains and other zinc-thiolate active sites. In relatively non-reductive intracellular local microenvironments, such as endoplasmic reticulum where low GSH:GSSG ratios close to 1 have been observed[3], the oxidized disulfide form may be sufficiently stable to undermine the primitive protein activity and kill cancerous cells.

Herein, we disclose a new targeted oxidation strategy (TOS II, **Fig. 1D**) based on special disulfide-type oxidants that may overcome both OD and DRT even in cytoplasm with high ratios of GSH:GSSG. The strategy essentially leverages specific intramolecular non-covalent interactions in proteins to stabilize the oxidized disulfide form and suppress DRT in GSH-rich microenvironments, potentially offering a new general pathway to inhibit cytosolic proliferation of RNA viruses. Quantum mechanical calculations suggest that it might be possible to develop such special disulfide-type oxidants selectively targeting thiol for a specific protein. Docking studies provide evidences to support a TOS II mechanism for the encouraging anti-2019-nCoV activities recently observed for two special disulfide oxidants, including FDA-approved anti-alcoholism drug disulfiram and PX-12[4]. A preliminary

list of promising TOS II drug candidates targeting thiol proteases M^{pro} and PL^{pro} of 2019-nCoV are proposed.

Results and Discussion

Chemical Principles Underlying TOS II and Potential Involvement of TOS II in Inhibition of 2019-nCoV

We first reasoned that there should be four distinctive types of disulfide oxidants with characteristic kinetic and thermodynamic behaviors in two competitive intracellular TOD/DRT reactions: 1) reduction of the disulfide oxidant by GSH to form a new small-molecule disulfide; and 2) reduction of the disulfide oxidant by protein thiol to form targeted protein disulfide (**Fig. 2A**). Type-I disulfide oxidants correspond to the situation where reaction 1 is both kinetically and thermodynamically more favorable than reaction 2, while type-II disulfide oxidants show complete reverse kinetic and thermodynamic behaviors. For type-III disulfide oxidants, although reaction 1 is kinetically more favorable than reaction 2, the opposite is true thermodynamically. In contrast to type III, vice versa is true for type IV. In principle, types II and III should be more suitable for TOS II than types I and IV in cytosolic microenvironments with high ratios of GSH:GSSG. Furthermore, type III may be less desirable than type II due to kinetics.
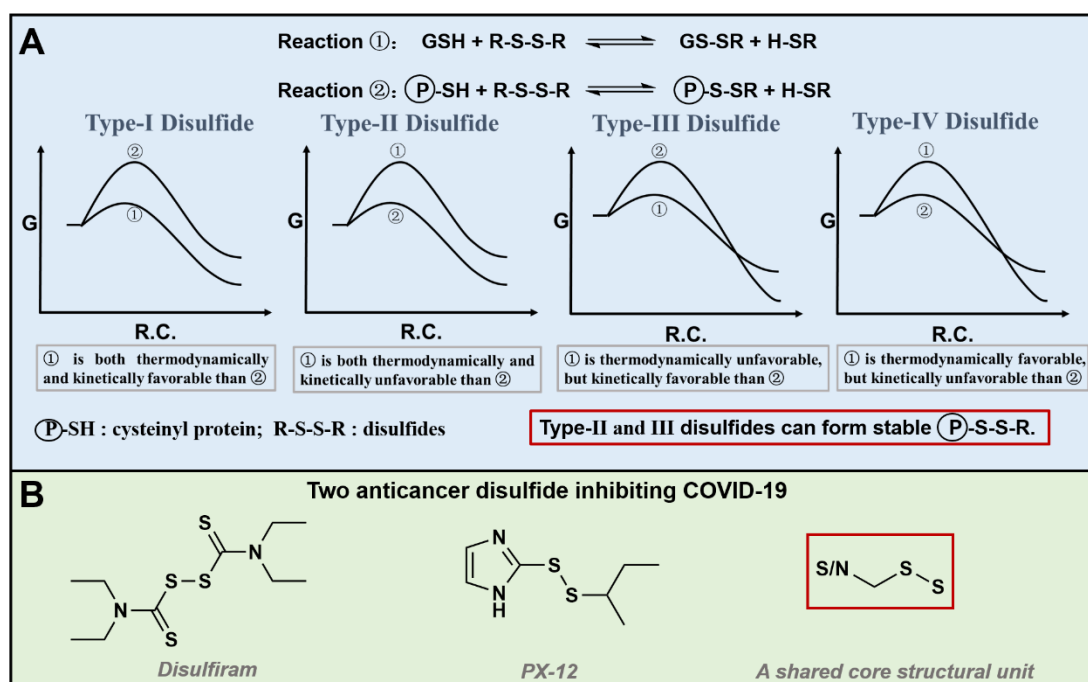
Figure 2. Schematics illustrating the principle for special disulfide-type oxidants: A. Four distinctive types of disulfide oxidants; B. Two suspected type II/III disulfides with recently reported anti-2019-nCoV activities.

Introduction of potential sites for non-covalent interactions at the targeted protein disulfide appears to be a natural approach to develop types II and III disulfide oxidants for TOS II. The encouraging cell-level anti-2019-nCoV activities of both disulfiram and PX-12[4] suggest the potential of using TOS II in inhibition of coronaviruses, where disulfide with hydrogen-bonding acceptor/donor (N or S) two bonds away is a shared core structural unit (**Fig. 2B**). . Such notion is supported by the observed inhibition of proteolytic activity of thiol protease M^{pro} of 2019-nCoV *in vitro* by both disulfides[4]. It should be noted that large excess amounts of a small cysteinyl fluogenic peptide with the sequence of MCA-AVLQSGFR-Lys(Dnp)-Lys-NH$_2$ was used as the substrate in the experiments, clearly

showcasing the remarkable abilities of both disulfides to discriminate between M^{pro} thiols and the substrate thiol. Earlier *in vitro* experimental observations and docking analysis of the inhibition effect of disulfiram onto proteolytic activities of thiol proteases of the caspase family[5] and coronoviruses including MERS-CoV and SARS-CoV[6] further suggest that such inhibition might be relevant to oxidation of the catalytically active thiol of M^{pro} to a disulfide.

Quantum-Mechanical Studies of Relevant Non-covalent Interactions

Using disulfiram and PX-12 as examples, we next performed quantum-mechanical calculations (Gaussian 09, Revision E.01) at the level of B3LYP/6-311+G(d,p) to gain fundamental insights into potential non-covalent interactions that may be involved in the formation of stable protein disulfides in general. Simplified model systems featured with relevant core functional groups were adapted to probe the interactions between the corresponding disulfide moieties covalently bonded to the proteins and various possible hydrogen-bonding donors in proteins, including the side chains of lysine, arginine, histidine, serine, threonine, asparagine, glutamine, tyrosine, and tryptophan (**Fig. 3A**). Model calculations were also performed to probe hydrogen-bonding complexes between PX-12 and various possible hydrogen bond acceptors in proteins, including histidine, serine, threonine, aspartic acid and glutamic acid (**Fig. 3D**). All optimized structures were confirmed to be real minima by frequency calculation. Notably, geometry optimization results indicate that thiocarbonyl S is preferred over the N as the hydrogen-bonding site in disulfiram.

Solvent effects were further calculated by SMD method to estimate the impacts of other non-covalent interactions including both electrostatic and non-electrostatic items. Gas phase (ε=1), benzene (ε=2.3), Z-1, 2-dichloroethene (ε=9.2), acetone (ε=20.5), acetonitrile (ε=35.7) and water (ε=78.4) were chosen to mimic various protein local microenvironments ranging from low polarity to high polarity. In principle, the dielectric environment in proteins should be closer to the nonpolar solvents than the polar ones. But the polar solvents were still studied here to interrogate the impacts of other non-covalent interactions implicitly. The calculated hydrogen-bonding enthalpies corrected by basis set superposition error (BSSE) were summarized in **Fig. 3B, Fig. 3C** and **Fig. 3E**.
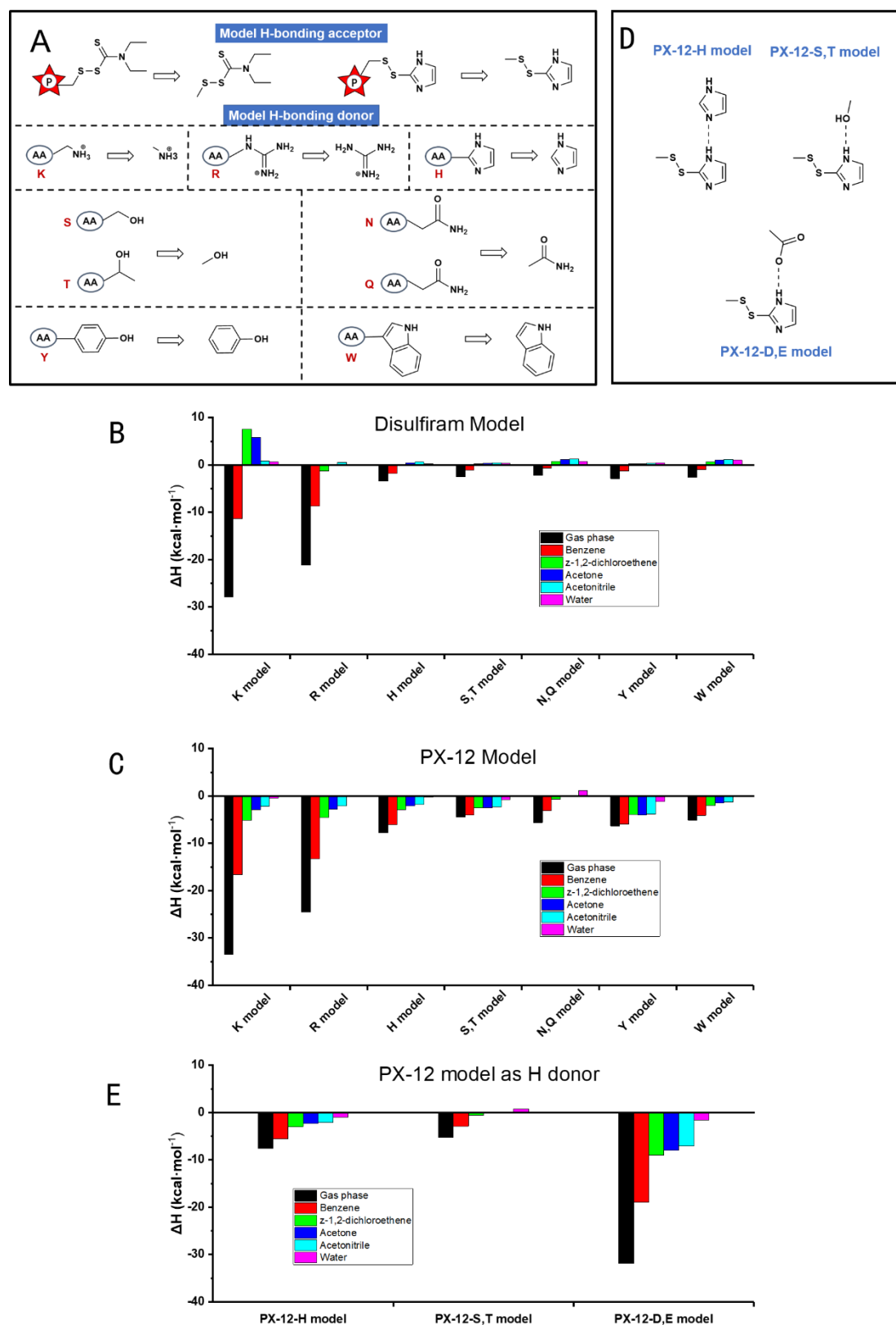
Figure 3. Schematics illustrating the principle for type II/III disulfide oxidants: A.

Adapted model molecules for potential interactions arising from hydrogen-accepting

disulfides covalently bonded to proteins and hydrogen-donating side chains of natural amino acids in proteins; Calculated hydrogen-bonding enthalpies with BSSE correction in various medium for model molecule of B: disulfiram and C: PX-12; D. Model complexes with PX-12 model molecule as a hydrogen donor; E. Calculated hydrogen-bonding enthalpies with BSSE for PX-12 model molecule as a hydrogen donor in various medium ranging from low polarity to high polarity.

The calculated results indicate that both disulfiram and PX-12 should be candidate type II/III disulfides. In general, hydrogen-bonding enthalpies decrease significantly as the polarity of the surrounding medium increases. Notably, the formation of hydrogen bonding complex is favored for most situations in nonpolar media. The impact of solvation onto the magnitude of hydrogen bonding enthalpy can be even larger than the impact of different types of hydrogen donors. Most calculated hydrogen bonding energies are in the range from *ca.* 2 kcal mol^{-1} to *ca.* 34 kcal mol^{-1} in non-polar media. It should be pointed out that each additional thermodynamic driving force of 1.4 kcal mol^{-1} from the non-covalent interactions at 37 ℃ would result in a 10-fold increase in the equilibrium constant toward the formation of the targeted protein disulfide. Although entropies were not considered here due to the inaccuracy in current entropy calculations, negligible contribution of entropy to hydrogen-bonding free energy can be envisioned for certain proteins where their tertiary structures have pre-organized hydrogen-bonding donors/acceptors in appropriate position and orientation. Under such circumstance, the absolute values of

the calculated enthalpies would be close to the corresponding free energies. Thus, it's reasonable to anticipate that appropriate non-covalent interactions can endow protein disulfides with the ability to resist DRT even in cytosolic microenvironments with high ratios of GSH:GSSG (*ca.* 30-100).

The different responses to the surrounding medium might underlie the different potencies in inhibitions of M[pro]/2019-nCoV between disulfiram and PX-12[1]. The model molecule for protein disulfide from PX-12 can form stable hydrogen-bonding complexes for most cases in both non-polar and polar solvents. In contrast, a non-polar environment is needed for the interaction between the disulfiram model molecule and the hydrogen donors to be energetically favorable. Therefore, although PX-12 may have stronger hydrogen-bonding interactions with proteins than disulfiram, the energetic driving force for diffusion from highly polar aqueous medium of cytoplasm into relatively non-polar proteins should be larger for disulfiram than PX-12, which may partially rationalize the higher inhibitory effects of disulfiram relative to PX-12 both *in vitro* and *in vivo*[4].

Additionally, the relative magnitude of the hydrogen-bonding enthalpies for the hydrogen-bonding donor follows the order of ammonium > guanidinium >> imidazole ~ phenol > indole ~ alcohol ~ amide for both model molecules of disulfiram and PX-12 in nonpolar media. In sharp contrast, the difference in hydrogen-bonding enthalpies becomes much smaller in polar media. Finally, the

interaction between PX-12 and hydrogen-bonding acceptor weakens as the order of carboxylate >> imidazole > alcohol in both polar and non-polar media. The large impact of hydrogen-bonding side chains of natural amino acids and polarity of the medium onto the hydrogen-bonding strength strongly suggests that it should be possible to develop type II/III disulfides selectively targeting thiol for a specific protein.

Potential TOS II Targets of 2019-nCoV and Docking Studies of Disulfides Potentially Targeting M^{pro} and PL^{pro} of 2019-nCoV via TOS II

Although experimental data have shown the oxidation of the catalytically active thiol of M^{pro} to disulfide as a potential mechanism for inhibition of 2019-nCoV, it's likely that oxidation of other thiol/zinc-thiolate sites by disulfiram/PX-12 might also play important roles in the inhibitions. As listed in Table 1, there are a few important proteins of 2019-nCoV containing targets for disulfides, including two thiol proteases M^{pro} and PL^{pro} as well as several proteins clearly involved in viral replication, such as RdRp, helicase, nsp10 and 3'-to-5' exonuclease. Notably, there are 12 cysteine residues in M^{pro} (Fig. 4A). Spike glycoprotein should also be a potential target since the abundant extracellular disulfides should be in corresponding thiol forms intracellularly. Considering the structural simplicity of disulfram and PX-12, the catalytic thiol of M^{pro} might just be one of the sites susceptible to TOD. ***But it should be emphasized that the disulfide bond in disulfiram can be reduced in the digestive processes and inner circulation, disabling its TOS II ability. Alternatively,***

the zinc-thiolate sites may be selectively oxidized via TOS I after coordination of the reduced product of disulfiram (DTC) with Cu(II) in vivo, potentially resulting in inhibition of the virus proliferation. Experimental evaluation of such possibility is recommended at least at cell level.

Table 1. Cysteine(s) in zinc fingers, active sites or disulfide bonds in proteins of 2019-nCoV that can be potentially oxidized by disulfides.

Accession	Protein name	Protein length	# of Cys	Cys in Zinc fingers (CF), active sites, disulfide bonds
YP_009724390.1	Spike	1273	40	disulfide bonds (C15-C136, C131-C166, C291-C301, C336-C361, C379-C432, C391-C525, C480-C488, C538-C590, C617-649, C662-C671, C738-C760, C743-C749, C840-C851, C1032-C1043, C1082-C1126)
YP_009725299.1	nsp3	1945	51	Zinc finger (C934, C937, C969, C971); active site in the PL^{pro} domain (C856)
YP_009725301.1	Mpro	306	12	active site (C145)
YP_009725306.1	nsp10	139	13	Zinc fingers (C74, C77, H83, C90; C117, C120, C128, C130)
YP_009725307.1	RdRp	932	29	Zinc fingers (H295, C301, C306, C310; C487, H642, C645, C646)
YP_009725308.1	helicase	601	26	Zinc fingers (C5, C8, C26, C29;C16, C19, H33, H39; C50, C55, C72, H75)
YP_009725309.1	3'-to-5' exonuclease	527	23	Zinc fingers (C207, C210, C226, H229;H257, C261, H264, C279; C452, C477, C484, H487)

To further investigate the mechanism of experimentally identified anti-2019-nCoV

drugs disulfiram and PX-12 via inhibition of M^{pro}, we performed covalent docking of the two drugs to M^{pro} (PDB ID: 6LU7[4]). First we focused on Cys145 – the catalytic cysteine of this thiol protease, and later we explored the possibility of other cysteines. In order to perform an ensemble docking, 200ns molecular dynamics simulation was performed on the crystal structure of M^{pro} (apo form) through Amber18, using ff14SB force field. Four M^{pro} conformations were obtained from trajectory clustering (100ns-200ns), based on conformations of residues in the ligand binding pocket. The four protein conformations and the two ligands were then prepared by Protein Preparation Wizard (Schrödinger 2019-2: Protein Preparation Wizard; Epik, Schrödinger, LLC, New York, NY, 2016; Impact, Schrödinger, LLC, New York, NY, 2016; Prime, Schrödinger, LLC, New York, NY, 2019) and LigPrep (Schrödinger 2019-2: LigPrep, Schrödinger, LLC, New York, NY, 2019), respectively. Covalent docking was performed by Glide (Schrödinger 2019-2: Glide, Schrödinger, LLC, New York, NY, 2019), disulfide bond is requested to form between ligand and the cysteine in active site of M^{pro} (Cys145). Representative docking poses were shown in Fig. 4B. Beyond the covalent disulfide bond, both disulfiram and PX-12 form good non-bonded interactions with M^{pro}, with disulfiram forming hydrogen bond with His163, and PX-12 forming hydrogen bonds with His164, and pi-pi stacking with His41. Next we explored the possibility of other cysteines in M^{pro} that can also be oxidized by disulfide drugs and may lead a negative allosteric modulation to the protease function of M^{pro}. Indeed there are a few sites that can accommodate the drugs quite well. Representative poses of disulfiram and PX-12 binding to Cys128 were

shown in Fig. 4C, both compounds form strong interactions with Lys5, and such interactions are further stabilized by Glu290, directly or indirectly.

To quantitatively compare these sites, the non-covalent-interacting disulfide cores were taken out of the docking structures (**Fig. S1**) for quantum-mechanical calculations at the level of B3LYP/6-311+G(d,p). It should be noted that these calculations might underestimate the strength of the non-covalent interactions because the surrounding amino acid residues might be actually flexible to adjust to better positions to interact with the disulfides than the docking structures. The calculated results show that the energetic benefits gained from the non-covalent interactions follow the order of C145/disulfiram < C145/PX-12 < C128/disulfiram ~ C128/PX-12 (**Table S1**). Again, non-polar media provide much stronger driving forces for the non-covalent interactions than polar media, further corroborating the notion that the different responses to the surrounding polarity might account for the higher anti-2019-nCoV activities of disulfiram than PX-12. To the end, the hydrophobicity of the ethyl substituents on N in disulfiram should play an important role. These results further support our hypothesis that non-covalent interactions contribute to the binding of these two molecules and the catalytically active C145 of M^{pro} should not be the sole targeting sites for TOS II. A mixture of both competitive and non-competitive inhibitions is expected for the kinetics of *in vitro* inhibitions of the proteolytic activities of M^{pro} of 2019-nCoV by disulfiram and PX-12. Further experimental verifications are suggested.
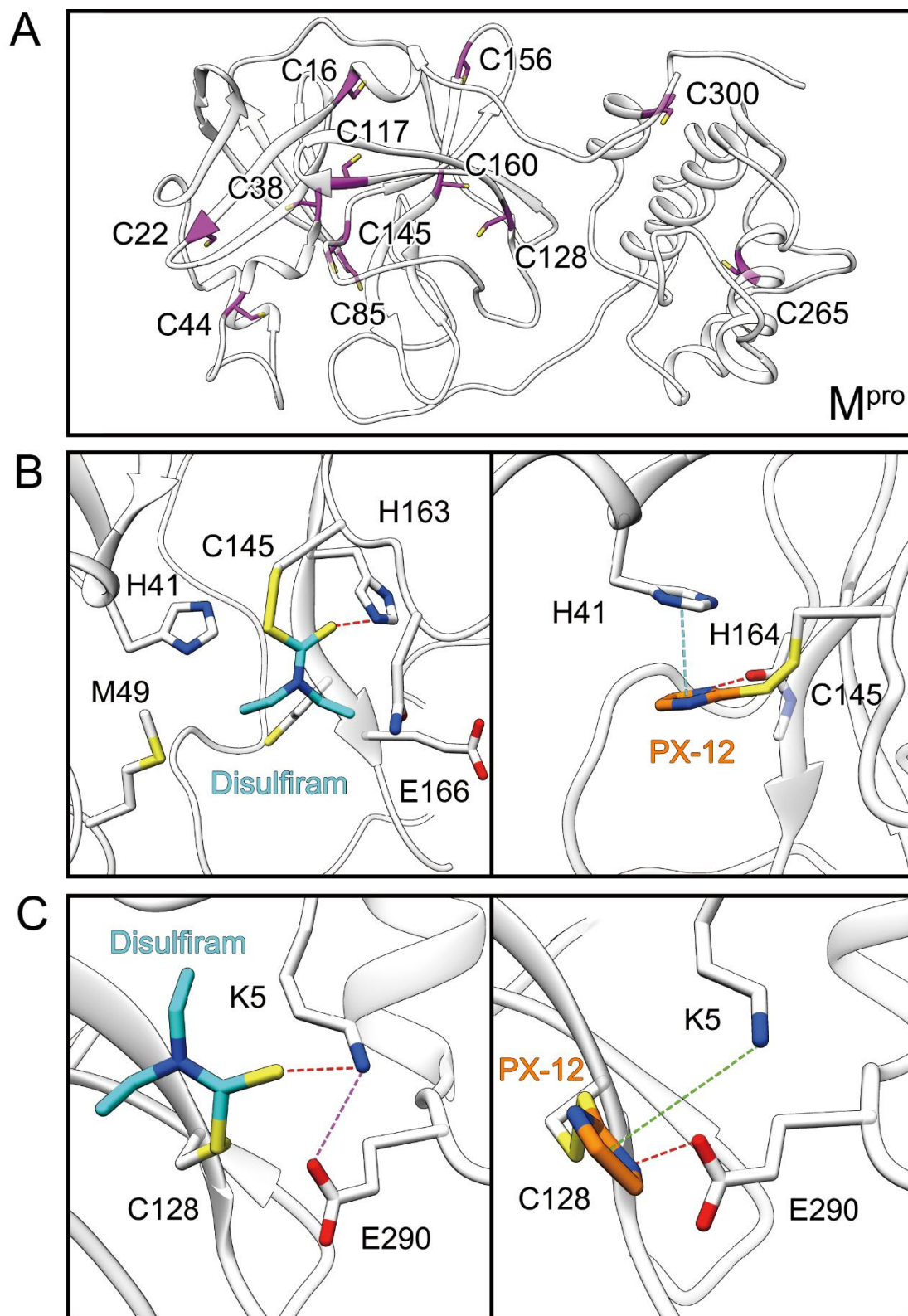
Figure 4. A) There are 12 cysteines in M^{pro}. B) Covalent docking poses of disulfiram and PX-12 in the active site of M^{pro}. C) Covalent docking poses of disulfiram and PX-12 at Cys128 of M^{pro}.

In order to identify more disulfide drug candidates, we performed large scale ensemble docking for both thiol proteases M^{pro} and PL^{pro}. Structure model of PL^{pro} was obtained from the C-I-TASSER website[7, 8]. Four conformations for each thiol protease obtained from MD sampling were used for docking. We built a large disulfide ligand library from filtering Enamine REAL set[9], one of the largest enumerated databases of synthetically feasible molecules which comply with "rule of 5" and Veber criteria. The focused ligand library has 32143 disulfides, and they were prepared by LigPrep for docking use.

Non-covalent docking was performed as the first step to pick ligands which could form good noncovalent interactions with the active site before covalent binding. This step aims to obtain ligands that are more likely to access the binding pocket, reducing the false positive rate of covalent docking due to high energy barrier for disulfide ligand to access the binding pocket. Then top 10% ranked ligands were used for further covalent docking. Our results showing that top ranked ligands tend to form polar interactions with His41 and Gln189 in M^{pro} (Fig. 5A), as well as His1017 and Trp851 in PL^{pro} (Fig. 5B). Finally, we proposed a list of molecules which may act as inhibitor of M^{Pro} or PL^{pro} based on TOS II through virtual screening (Tables S1 and S2). Unfortunately, further searching of candidate inhibitors are still limited by the lack of crystal structure for relevant proteins other M^{pro} and PL^{pro}.
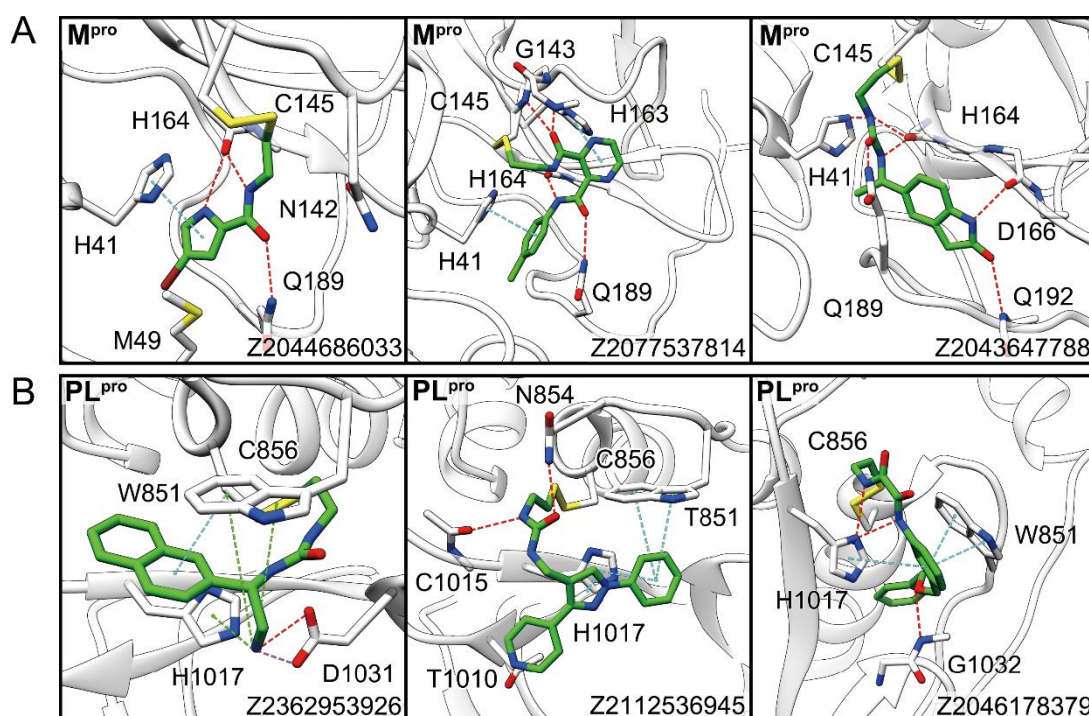
Figure 5. Selected top ranked hits for M^{pro} (A) and PL^{pro}(B) from a two-step virtual screening: first non-covalent docking and then covalent docking.

Conclusions:

In summary, we have described the fundamental principles to overcome the intracellular reductive-protection mechanism for potential therapeutic purposes via TOS II. The encouraging cell-level anti-2019-nCoV activities of both disulfiram and PX-12 suggest the potential of using TOS II in inhibition of coronaviruses. In particular, disulfiram is a simple and cheap drug that has been approved by FDA for anti-alcoholism purpose for *ca.* 70 years. Given the urgent needs of therapeutic methods to treat 2019-nCoV in the ongoing international outbreak, it's of great significance to further explore its potential anti-2019-nCoV activity at clinical levels. *However, further animal evaluations and clinical trials to develop appropriate methods to prevent the gradual degradation of disulfiram in digestive*

processes/inner circulation and allow its transport to infected tissues is recommended if its potential anti-2019-nCoV activity via TOS II would be leveraged to a large extent.

In addition to potential interference of cytosolic proliferations of coronaviruses, TOS II might also be envisioned to trigger other significant physiological consequences such as inhibiting protein ubiquitinations via oxidation of the active cysteinyl thiols of ubiquitin-activating enzyme E1 and ubiquitin-conjugating enzyme E2 to form stable disulfides that can resist the reductive environments in cells. Considering the ubiquity of thiol/zinc-thiolate sites in proteins and their important biological roles, we hope that more research attention can be devoted to the development of TOS II drugs for various therapeutic applications.

Supporting Information. **Figure S1, Tables S1, S2, S3.**

Acknowledgement

Notes

The authors declare no competing financial interest.

REFERENCES

1. Xu, L. Y.; Xu, J. L.; Zhu, J. W.; Yao, Z. J.; Yu, N.; Deng, W.; Wang, Y.; Lin, B. L., Universal Anticancer Cu(DTC)(2) Discriminates between Thiols and Zinc(II) Thiolates Oxidatively. *Angewandte Chemie-International Edition* **2019,** *58* (18), 6070-6073.

2. Webster, K. A.; Prentice, H.; Bishopric, N. H., Oxidation of zinc finger transcription factors: Physiological consequences. *Antioxidants & Redox Signaling* **2001,** *3* (4), 535-548.

3. Hwang, C.; Sinskey, A. J.; Lodish, H. F., Oxidized Redox State of Glutathione in the Endoplasmic-Reticulum. *Science* **1992,** *257* (5076), 1496-1502.

4. Jin, Z.; Du, X.; Xu, Y.; Deng, Y.; Liu, M.; Zhao, Y.; Zhang, B.; Li, X.; Zhang, L.; Duan, Y.; Yu, J.; Wang, L.; Yang, K.; Liu, F.; You, T.; Liu, X.; Yang, X.; Bai, F.; Liu, H.; Liu, X.; Guddat, L. W.; Xiao, G.; Qin, C.; Shi, Z.; Jiang, H.; Rao, Z.; Yang, H., Structure-based drug design, virtual screening and high-throughput screening rapidly identify antiviral leads targeting COVID-19. **2020**, 2020.02.26.964882.

5. Nobel, C. S. I.; Kimland, M.; Nicholson, D. W.; Orrenius, S.; Slater, A. F. G., Disulfiram is a potent inhibitor of proteases of the caspase family. *Chemical Research in Toxicology* **1997,** *10* (12), 1319-1324.

6. Lin, M. H.; Moses, D. C.; Hsieh, C. H.; Cheng, S. C.; Chen, Y. H.; Sun, C. Y.; Chou, C. Y., Disulfiram can inhibit MERS and SARS coronavirus papain-like proteases via different modes. *Antiviral*

Research **2018,** *150*, 155-163.

7.   Zhang, C.;   Zheng, W.;   Huang, X.;   Bell, E. W.;   Zhou, X.; Zhang, Y., Protein structure and sequence re-analysis of 2019-nCoV genome does not indicate snakes as its intermediate host or the unique similarity between its spike protein insertions and HIV-1. **2020**, 2020.02.04.933135.

8.   Zhang, C.;   Mortuza, S. M.;   He, B.;   Wang, Y.;   Zhang, Y. J. P. S. F.; Bioinformatics, Template-based and free modeling of I-TASSER and QUARK pipelines using predicted contact maps in CASP12. **2017,** *86 Suppl 1* (S10).

9.   Lyu, J.;   Wang, S.;   Balius, T. E.;   Singh, I.;   Levit, A.;   Moroz, Y. S.;   O'Meara, M. J.;   Che, T.; Algaa, E.;   Tolmachova, K.;   Tolmachev, A. A.;   Shoichet, B. K.;   Roth, B. L.; Irwin, J. J., Ultra-large library docking for discovering new chemotypes. *Nature* **2019,** *566* (7743), 224-229.

Supporting Information

Figure S1. Core structures taken from docking analysis for quantum-mechanical calculations.
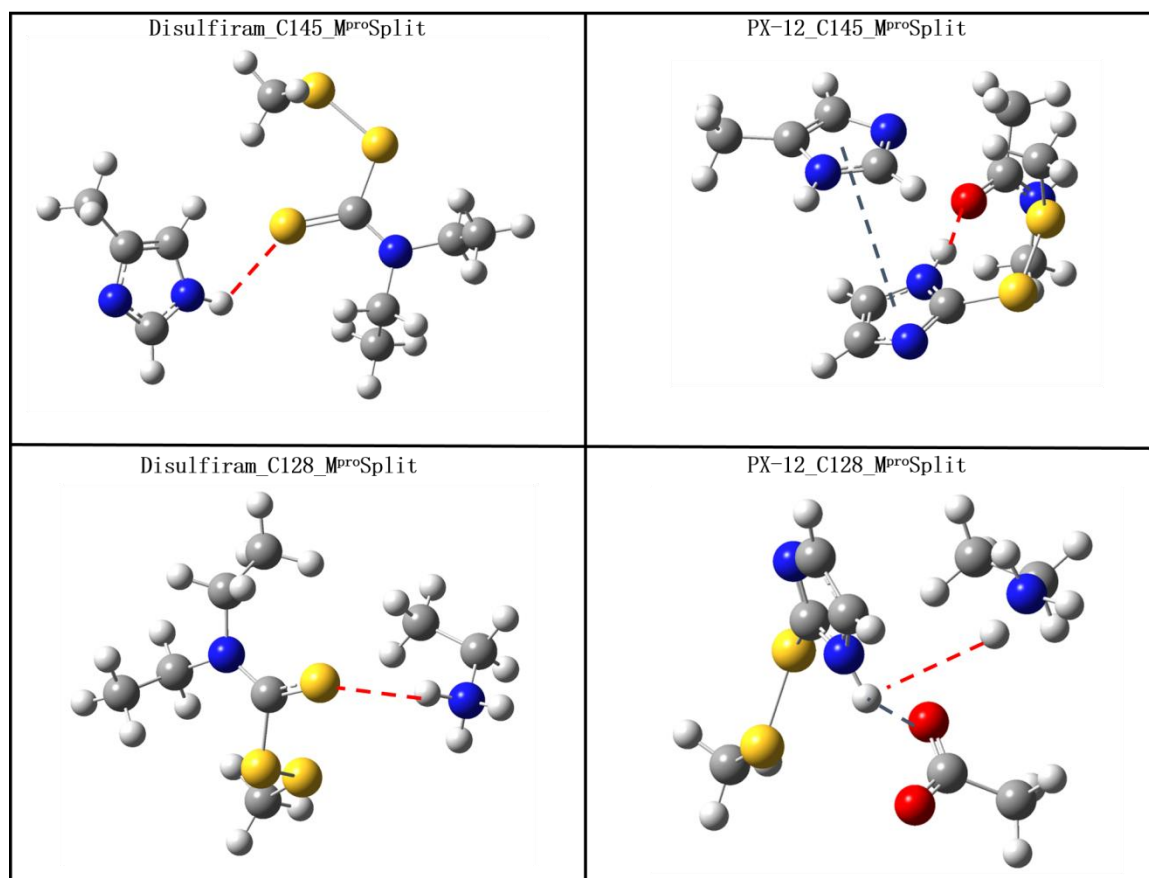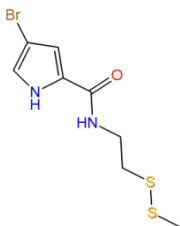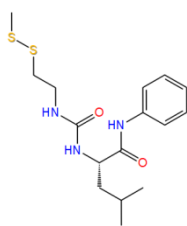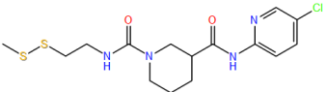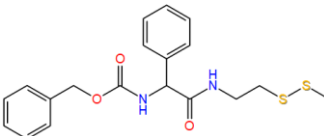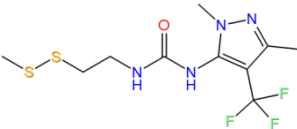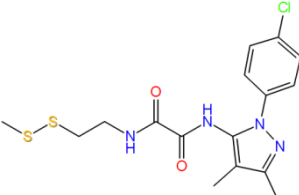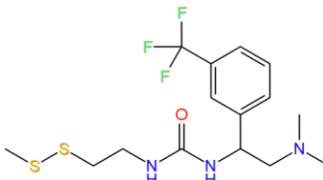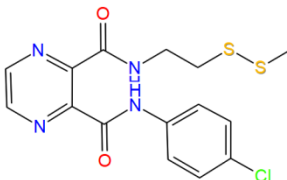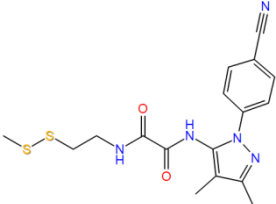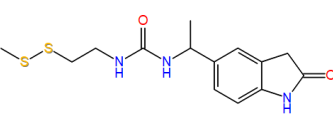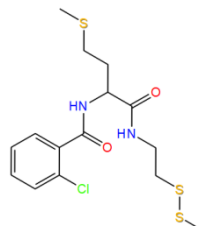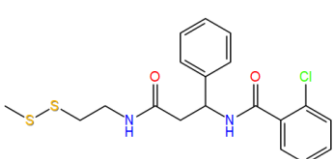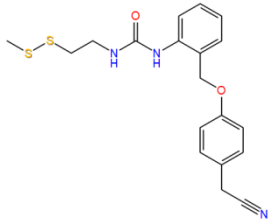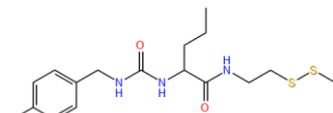
Table S1. Calculated non-covalent interaction energies in various media (corrected with BSSE, unit kcal·mol^{-1})

	disulfiram_C145_M^{pro}Split	PX-12_C145_M^{pro}Split	disulfiram_C128_M^{pro}Split	PX-12_C128_M^{pro}Split
Gas Phase	-0.46	-6.77	-18.51	-13.62
Benzene	1.28	-1.75	-6.26	-6.64
z-1,2-dichloroethene	2.28	1.05	0.91	-1.03
Acetone	2.48	1.61	2.23	-0.29
Acetonitrile	2.49	1.76	2.63	0.17
Water	1.88	0.98	1.91	2.19

Table S2. Selected top ranked docking results of M^pro.

EnamineID	Structure	EnamineID	Structure
Z2044686033		PV-002085776328	
Z2121597469		Z2077557884	
PV-002407528684		Z2046179495	
PV-002359354653		Z2077537814	
Z2046180551		Z2043647788	
Z2044679216		Z2044679130	
Z2054127313		Z2044681428	

Z2046180547
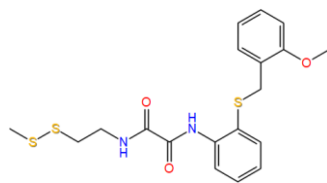
PV-002431516373
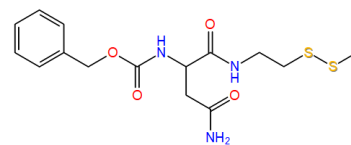
PV-002089654013
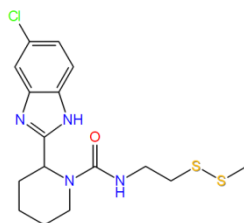
PV-002500806505
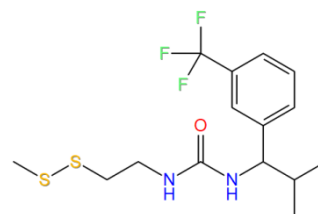
PV-002181388899
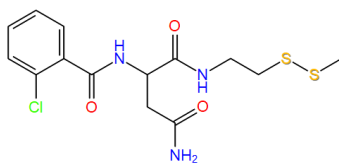
Z2044681760
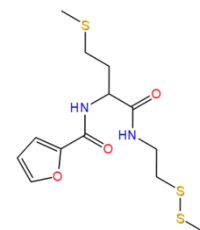
Z2043901219
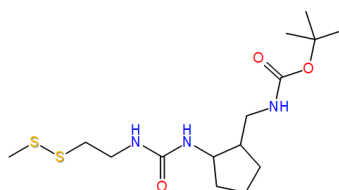
PV-002268103046
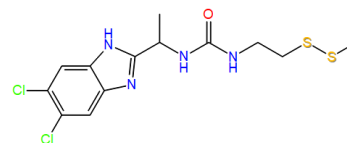
Z2044685197
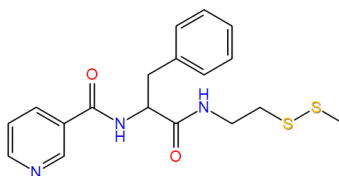
Z2044681489
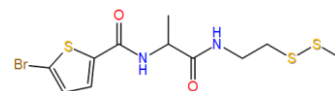
Z2044683461
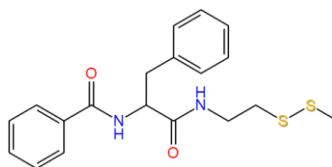
Z2926448105
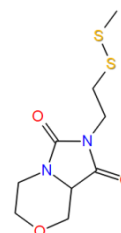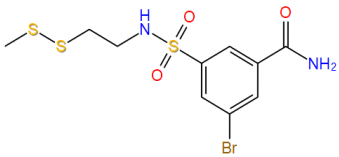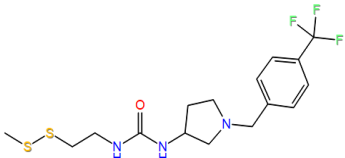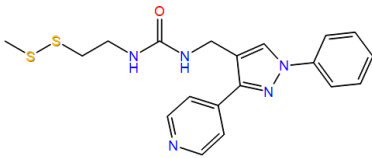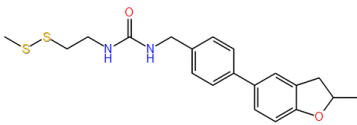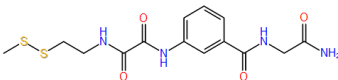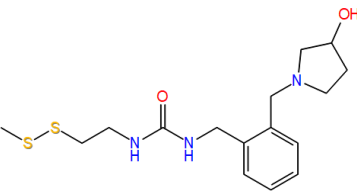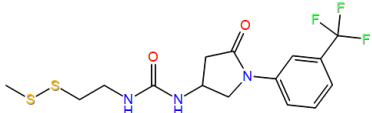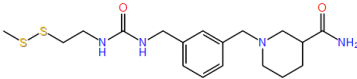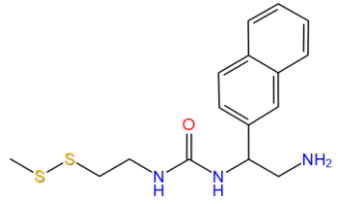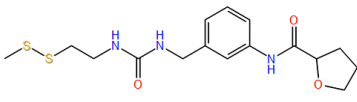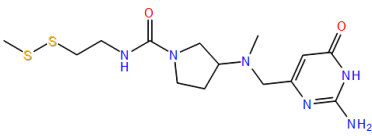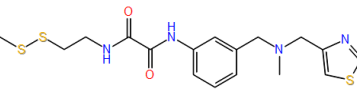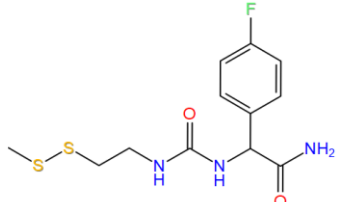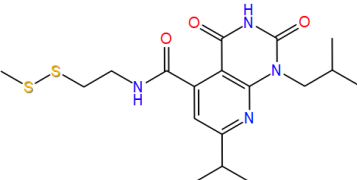
Table S3. Selected top ranked docking results of PL^pro.

EnamineID	Structure	EnamineID	Structure
Z2043114325		Z2044111862	
Z2112536945		PV-002420985695	
Z2046178634		Z2043970454	
Z2043911055		Z2044123382	
Z2362953926		Z2043836263	
Z2044107946		Z2046180029	
Z2044109064		Z2077540817	

Z2046178379
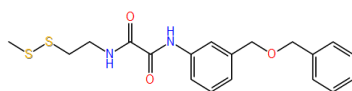
Z2044123024
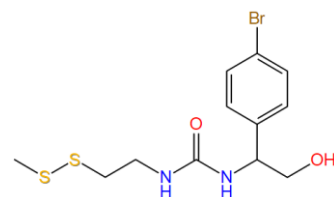
Z2121587734
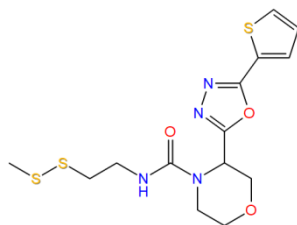
Z2121603746
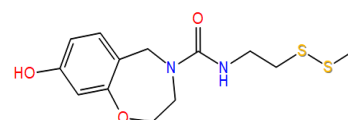
Z2100541651
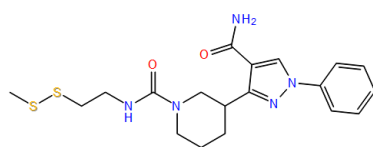
Z2044122862
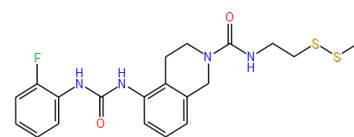
Z2362954041
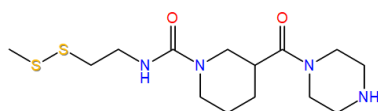
Z2093340626
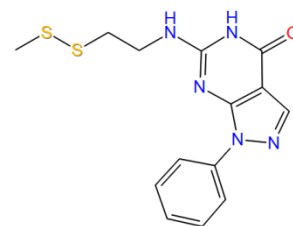
Z2183829798
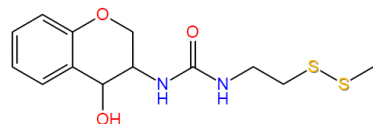
Z3211532847
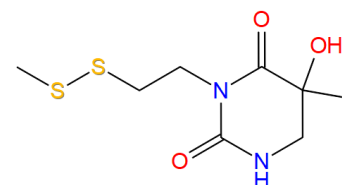
Z2077545489
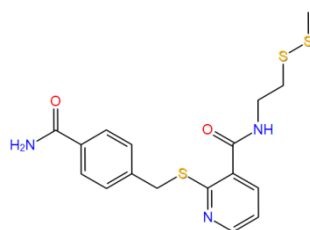
Z2044733383
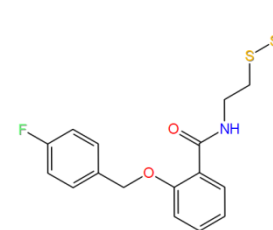
Z2044108077

Z2355154234

Z3211532903

Z2044678984